Article:
Huang, B., Lyu, Z., Qian, Q. et al. (20 more authors) (2022) NUDT1 promotes the accumulation and longevity of CD103+ TRM cells in primary biliary cholangitis. Journal of Hepatology, 77 (5). pp. 1311-1324. ISSN 0168-8278

https://doi.org/10.1016/j.jhep.2022.06.014

Research Article
DILI, Autoimmune, Cholestatic and Genetic Diseases

JOURNAL OF HEPATOLOGY

NUDT1 promotes the accumulation and longevity of CD103$^+$ T_{RM} cells in primary biliary cholangitis

Graphical abstract

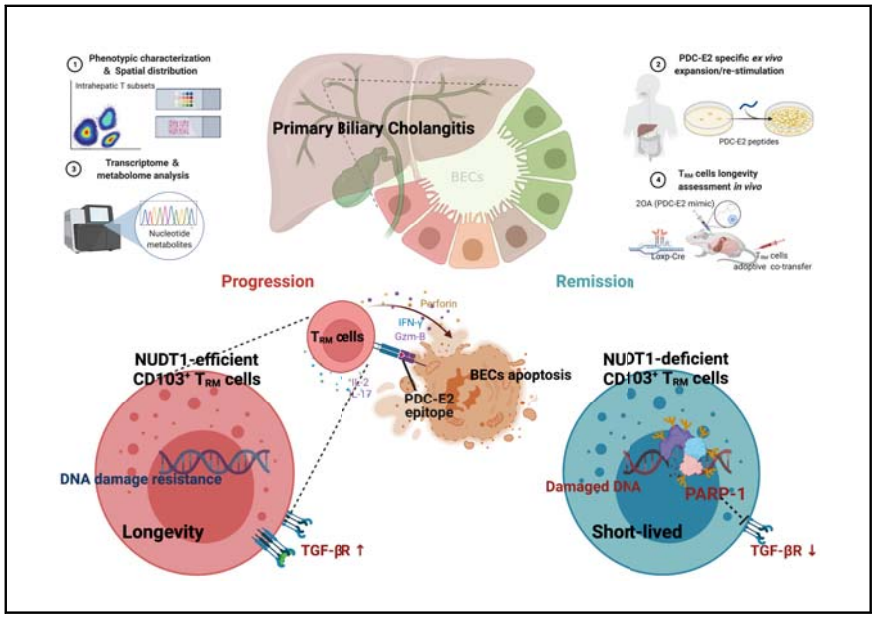

Highlights

- CD103$^+$ T_{RM} cells are the dominant population of PDC-E2-specific autoreactive cytotoxic T cells in livers of patients with PBC.
- CD103$^+$ T_{RM} cells exhibit cytotoxicity against autologous cholangiocytes in PBC.
- Upon antigenic stimulation, metabolic reprogramming and DNA damage response of CD103$^+$ T_{RM} cells is orchestrated by NUDT1.
- NUDT1-dependent DNA damage resistance promotes long-term survival of CD103$^+$ T_{RM} cells via PARP1-TGFβ-Smad axis.

Authors

Bingyuan Huang, Zhuwan Lyu, Qiwei Qian, …, M. Eric Gershwin, Zhengrui You, Xiong Ma

Correspondence

maxiongmd@hotmail.com (X. Ma), youzhengrui@126.com (Z. You), megershwin@ucdavis.edu (M.E. Gershwin).

Lay summary

Primary biliary cholangitis (PBC) is a rare inflammatory condition of the bile ducts. It can be treated with ursodeoxycholic acid, but a large percentage of patients respond poorly to this treatment. Liver-infiltrating memory CD8$^+$ T cells recognizing the PDC-E2 immunodominant epitope are critical in the pathogenesis of PBC. We identifed the key pathogenic CD8$^+$ T cell subset, and worked out the mechanisms of its hyperactivation and longevity, which could be exploited therapeutically.

https://doi.org/10.1016/j.jhep.2022.06.014
 J. Hepatol. 2022, 77, 1311–1324

Research Article
DILI, Autoimmune, Cholestatic and Genetic Diseases

JOURNAL OF HEPATOLOGY

NUDT1 promotes the accumulation and longevity of CD103$^+$ T_{RM} cells in primary biliary cholangitis

Bingyuan Huang[1,#], Zhuwan Lyu[1,#], Qiwei Qian[1,#], Yong Chen[1], Jun Zhang[1], Bo Li[1], Yikang Li[1], Jubo Liang[1], Qiaoyan Liu[1], You Li[1], Ruiling Chen[1], Min Lian[1], Xiao Xiao[1], Qi Miao[1], Qixia Wang[1], Jingyuan Fang[1], Zhexiong Lian[2], Yanmei Li[3], Ruqi Tang[1], Thomas Helleday[4,5], M. Eric Gershwin[6,*,†], Zhengrui You[1,*,†], Xiong Ma[1,*,†]

[1]*Division of Gastroenterology and Hepatology, Key Laboratory of Gastroenterology and Hepatology, Ministry of Health, State Key Laboratory for Oncogenes and Related Genes, Renji Hospital, School of Medicine, Shanghai Jiao Tong University, Shanghai Institute of Digestive Disease, 145 Middle Shandong Road, Shanghai 200001, China;* [2]*Chronic Disease Laboratory, Institutes for Life Sciences and School of Medicine, South China University of Technology, Guangzhou 510006, China;* [3]*Department of Clinical Immunology and Rheumatology, Tianjin Medical University General Hospital, Tianjin, China;* [4]*Science for Life Laboratory, Department of Oncology-Pathology, Karolinska Institute, 171 76 Stockholm, Sweden;* [5]*Weston Park Cancer Centre, Department of Oncology and Metabolism, University of Sheffield, Sheffield S10 2RX, United Kingdom;* [6]*Division of Rheumatology, Department of Medicine, Allergy and Clinical Immunology, University of California at Davis, Davis, CA, USA*

Background & Aims: Pyruvate dehydrogenase (PDC)-E2 specific CD8$^+$ T cells play a leading role in biliary destruction in PBC. However, there are limited data on the characterization of these autoantigen-specific CD8$^+$ T cells, particularly in the liver. Herein, we aimed to identify pathogenic intrahepatic CD8$^+$ T-cell subpopulations and investigate their immunobiology in PBC.

Methods: Phenotypic and functional analysis of intrahepatic T-cell subsets were performed by flow cytometry. CD103$^+$ T_{RM} cell frequency was evaluated by histological staining. The transcriptome and metabolome were analyzed by RNA-seq and liquid chromatography-mass spectrometry, respectively. Cytotoxicity of T_{RM} cells against cholangiocytes was assayed in a 3D organoid co-culture system. Moreover, the longevity (long-term survival) of T_{RM} cells *in vivo* was studied by 2-octynoic acid-BSA (2OA-BSA) immunization, *Nudt1* conditional knock-out and adoptive co-transfer in a murine model.

Results: Intrahepatic CD103$^+$ T_{RM} (CD69$^+$CD103$^+$CD8$^+$) cells were significantly expanded, hyperactivated, and potentially specifically reactive to PDC-E2 in patients with PBC. CD103$^+$ T_{RM} cell frequencies correlated with clinical and histological indices of PBC and predicted poor ursodeoxycholic acid response. NUDT1 blockade suppressed the cytotoxic effector functions of CD103$^+$ T_{RM} cells upon PDC-E2 re-stimulation. NUDT1 overexpression in CD8$^+$ T cells promoted tissue-residence programming *in vitro*; inhibition or knockdown of NUDT1 had the opposite effect. Pharmacological blockade or genetic deletion of NUDT1 eliminated CD103$^+$ T_{RM} cells and alleviated cholangitis in mice immunized with 2OA-BSA. Significantly, NUDT1-dependent DNA damage resistance potentiates CD8$^+$ T-cell tissue-residency via the PARP1-TGFβR axis *in vitro*. Consistently, PARP1 inhibition restored NUDT1-deficient CD103$^+$ T_{RM} cell durable survival and TGFβ-Smad signaling.

Conclusions: CD103$^+$ T_{RM} cells are the dominant population of PDC-E2-specific CD8$^+$ T lymphocytes in the livers of patients with PBC. The role of NUDT1 in promoting pathogenic CD103$^+$ T_{RM} cell accumulation and longevity represents a novel therapeutic target in PBC.

Lay summary: Primary biliary cholangitis (PBC) is a rare inflammatory condition of the bile ducts. It can be treated with ursodeoxycholic acid, but a large percentage of patients respond poorly to this treatment. Liver-infiltrating memory CD8$^+$ T cells recognizing the PDC-E2 immunodominant epitope are critical in the pathogenesis of PBC. We identifed the key pathogenic CD8$^+$ T cell subset, and worked out the mechanisms of its hyperactivation and longevity, which could be exploited therapeutically.

Keywords: Primary biliary cholangitis; PDC-E2; Tissue-resident memory T cells; NUDT1; DNA damage response.
Received 10 November 2021; received in revised form 21 May 2022; accepted 7 June 2022; available online 23 June 2022

* Corresponding authors. Addresses: Renji Hospital, School of Medicine, Shanghai Jiao Tong University, Shanghai Institute of Digestive Disease, 145 Middle Shandong Road, Shanghai 200001, China (X. Ma), or Division of Rheumatology, Department of Medicine, Allergy and Clinical Immunology, University of California at Davis, Davis, CA, USA (M.E. Gershwin).
E-mail addresses: maxiongmd@hotmail.com (X. Ma), youzhengrui@126.com (Z. You), megershwin@ucdavis.edu (M.E. Gershwin).
[#] BH, ZL and QQ joint first co-authorship.
[†] MEG, ZY and XM joint last co-authorship.
https://doi.org/10.1016/j.jhep.2022.06.014

Introduction

Patients with primary biliary cholangitis (PBC) develop a multilineage response to a highly restricted peptide of the E2 component of pyruvate dehydrogenase (PDC-E2) including antimitochondrial antibodies and autoreactive T-cell responses.[1] CD8$^+$ cytotoxic T lymphocytes (CTLs) are thought to be directly involved in the apoptosis of biliary epithelial cells (BECs) during PBC progression.[2] Memory CD8$^+$ T cells recognizing the PDC-E2 immunodominant epitope are found only in patients with PBC and are significantly enriched in the liver compared to peripheral blood, highlighting their disease- and organ-specificity.[3]

Treatment of PBC has been dominated by routine ursodeoxycholic acid (UDCA) therapy, which is ineffective in 30-40% of patients.[4] High-risk patients would probably benefit from early combined treatment with UDCA and immunotherapies.[5,6] Despite the lack of uniform success with targeted therapies based on autoantigen-reactive CTLs in PBC to date, this approach remains promising.[7] Therefore, phenotypic and functional characterization of the pathogenic cytotoxic T-cell subsets is urgently needed.[3,8] Increasing evidence support that relapsed/refractory autoimmune diseases are partially driven by tissue-resident memory $CD8^+$ T (T_{RM}) cells, a recently identified T-cell subset that lodges permanently in non-lymphoid tissues without recirculating.[9,10]

T_{RM} cells often express CD69, integrins CD49a and CD103 that mediate long-term retention within tissues.[11,12] T_{RM} cells within the human liver can be further divided by CD103 expression into 2 subpopulations exhibiting substantial functional differences: $CD103^-$ T_{RM} cells ($CD69^+CD103^-CD8^+$ T cells) and $CD103^+$ T_{RM} cells ($CD69^+CD103^+CD8^+$ T cells).[13,14] Upon antigen or cytokine stimulation, $CD103^+$ T_{RM} cells are stronger effectors than $CD103^-$ T_{RM} cells, exhibiting robust inflammatory sentinel activity and long-term survival (longevity) in diseased livers.[13,15] Interestingly, in patients with chronic HBV infection, $CD103^-$ T_{RM} cells have specificity for both hepatotropic and non-hepatotropic viruses, whereas $CD103^+$ T_{RM} subsets are only HBV-specific cells. Moreover, antigen-nonspecific activation of liver-resident $CD8^+$ T cells contributes to inflammation in HDV.[16] Beyond the antigen specificity, $CD103^+$ T_{RM} cells also exhibit distinct functional heterogeneity and plasticity. In cholangiocarcinoma, $CD103^+$ T_{RM} cells express prominent exhaustion-related checkpoint receptors, but still retain a T-bet^{high} $Eomes^{low}$ population with reinvigoration potential.[17] The balance between $CD103^+$ T_{RM} and exhausted T cells is also predictive of outcomes in hepatocellular carcinoma.[18]

Herein, we report that in PBC, expanded $CD103^+$ T_{RM} cells are the dominant intrahepatic population of PDC-E2-specific autoreactive CTLs. Upon antigenic stimulation, $CD103^+$ T_{RM} cells require nucleoside diphosphate X hydrolase 1 (NUDT1), a nucleotide pool sanitizing enzyme, to improve tolerance to oxidative stress derived from metabolic reprogramming. Genetic deletion or pharmacological blockade of NUDT1 eliminates $CD103^+$ T_{RM} cells in our PBC murine model and is accompanied by reduced portal inflammation. Significantly, NUDT1-dependent oxidative DNA damage resistance imprints $CD8^+$ T-cell tissue-residency via the PARP1-TGFβR axis *in vitro*. Consistently, PARP1 inhibition restores NUDT1-deficient $CD103^+$ T_{RM} cell survival and TGFβ-Smad signaling both *in vitro* and *in vivo*.

Materials and methods

Patients and study samples

Demographic and clinical features of study participants are included in Table S1 and Table S2. All individuals were enrolled in Shanghai Renji Hospital and provided written, informed consent. The study was carried out under the principles of the Declaration of Helsinki and approved by the research ethics boards of Renji Hospital, Shanghai Jiao Tong University.

Animal studies

We generated *Nudt1*$^{flox/flox}$ mice using a standard CRISPR/Cas9-mediated gene editing strategy. To specifically delete the NUDT1 from T cells, *Nudt1*$^{flox/flox}$ mice were bred with a CD4-Cre transgenic mouse strain to generate the *Nudt1*$^{\triangle CD4}$ mice on a C57BL/6 background. Procedure details of 2OA immunization and T-cell adoptive transfer/co-transfer can be found in the supplementary methods.

Additional information on the materials and methods used can be found in the supplementary methods and supplementary CTAT table.

Results

$CD103^+$ T_{RM} cells are significantly expanded and hyperactivated in PBC

A significantly increased frequency of $CD103^+$ T_{RM} cells ($CD69^+CD103^+CD8^+$ T cells) among liver-infiltrating $CD8^+$ T cells was observed in patients with PBC compared to healthy controls (HCs) (Fig. 1A). $CD103^+$ T_{RM} cells from patients with PBC demonstrated a higher expression of PD-1 and CXCR3 (Fig. 1B) and secreted significantly more cytokines including granzyme-B, IFN-γ, IL-2 and IL-17 (Fig. 1C) than those of HCs, indicating $CD103^+$ T_{RM} cells were hyperactivated with enhanced effector functions in PBC. $CD103^+$ T_{RM} cells also exhibited significantly higher proliferation/self-renewal related transcription factors, including Ki-67 and TCF-1, but simultaneously expressed higher exhaustion-associated TOX (Fig. 1C). The seemingly contradictory transcriptional program revealed a substantial internal heterogeneity of $CD103^+$ T_{RM} cell phenotypes.

Autoreactivity of $CD103^+$ T_{RM} cells is potentially specific to PDC-E2 in PBC

We sorted liver-infiltrating $CD103^+$ T_{RM} ($CD69^+CD103^+CD8^+$) cells, $CD103^-$ T_{RM} ($CD69^+CD103^-CD8^+$) cells and "non-resident" $CD69^-CD103^-CD8^+$ T cells from liver explants of HLA-A^*0201^+ patients with PBC to expand peptide-specific CTL lines with PDC-$E2_{159-167}$ peptide. Distinct populations of the PDC-$E2_{159-167}$ $tetramer^+$ $CD8^+$ T cells were detected after a 12–14-day expansion of paired $CD103^+$ and $CD103^-$ T_{RM} cells (Fig. 1D), while PDC-$E2_{159-167}$ $tetramer^+$ $CD8^+$ T cells derived from the $CD69^-CD103^-CD8^+$ counterpart were still undetectable.

The frequency of PDC-E2 peptide-specific T-cell precursors before expansion was estimated by the number of cell divisions. The average frequency of PDC-$E2_{159-167}$-specific reactive cells among liver-infiltrating $CD103^+$ T_{RM} cells was significantly higher (over 3-fold) than that among $CD103^-$ T_{RM} cells (Fig. 1E). Combining with their respective proportions in liver-infiltrating $CD8^+$ T cells, more than 60% of the PDC-E2 reactive $CD69^+CD8^+$ T cells were $CD103^+$ T_{RM} cells (Fig. 1F). Moreover, $CD103^+$ T_{RM} cells sorted from all HLA-A^*0201^+ HCs and disease controls failed to expand $tetramer^+$ cells at detectable and comparable levels (Fig. S1B). Upon PDC-E2 peptide stimulation, $CD103^+$ T_{RM} cells produced more IFN-γ and granzyme-B compared to paired $CD103^-$ T_{RM} cells (Fig. 1G). The prevalence of autoantigen-reactive T cells in $CD103^-$ and $CD103^+$ T_{RM} cell subsets and their differential antigen responsiveness was also confirmed by measurement of IFN-γ in supernatants (Fig. 1H; Fig. S1C). As expected, $CD103^+$ T_{RM} cells from HCs and disease controls did not respond to the stimulation (Fig. S1D). Overall, these findings reflect that $CD103^+$ T_{RM} cells are the major population of PDC-E2-specific autoreactive $CD8^+$ T lymphocytes in the livers of patients with PBC.

$CD103^+$ T_{RM} cells are clinically relevant in PBC

We confirmed that $CD103^+$ T_{RM} cells accumulate around damaged interlobular bile ducts in the peri-portal areas by

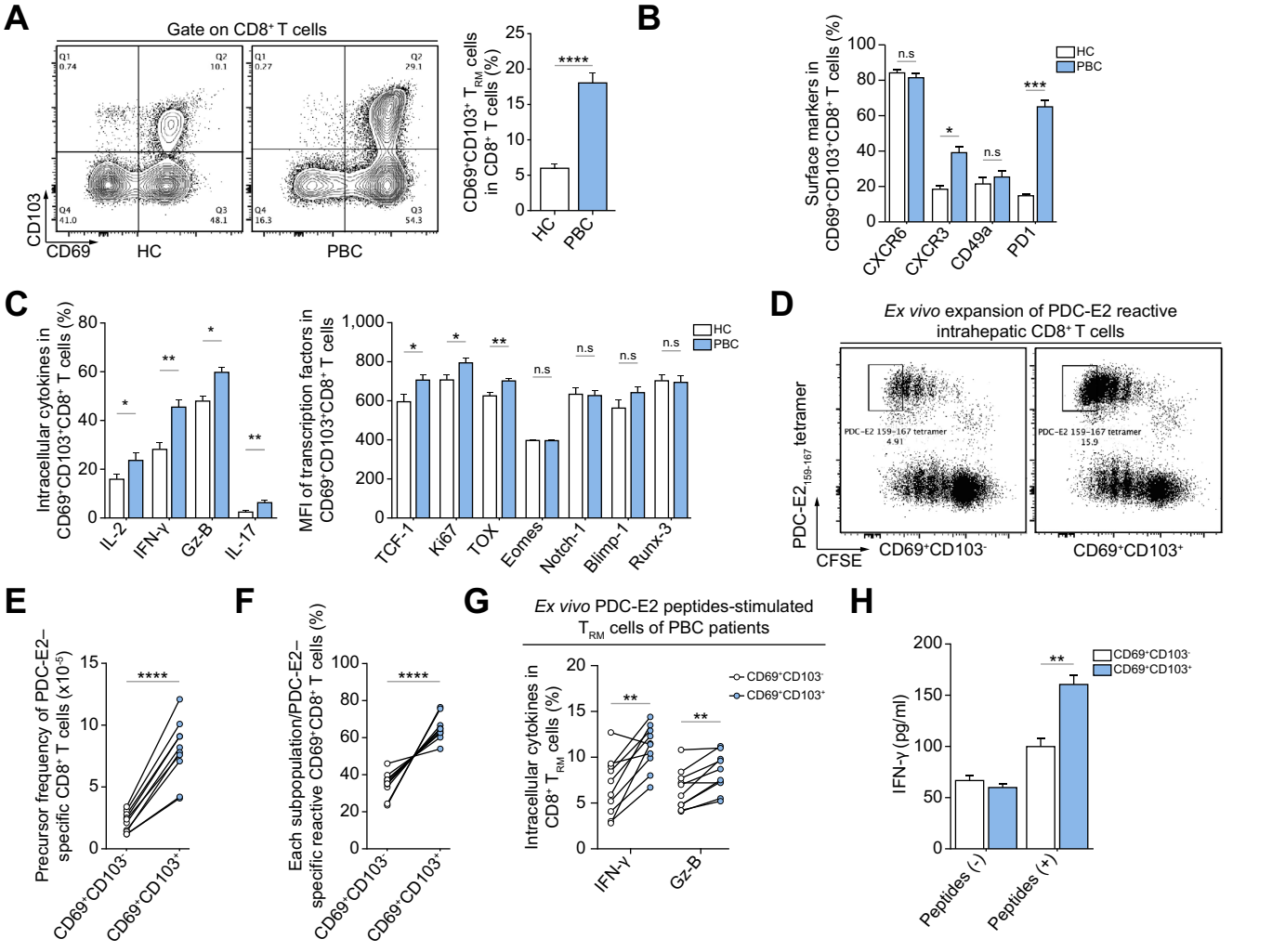

Fig. 1. Phenotype and autoantigen-specificity of CD103$^-$ and CD103$^+$ T_{RM} cells in PBC. (A) Frequency of liver-infiltrating CD103$^+$ T_{RM} cells in HCs (n = 15) and patients with PBC (n = 18). (B and C) Expression of surface markers (B), intracellular cytokines and transcription factors (C) in liver-infiltrating CD103$^+$ T_{RM} cells from HCs (n = 15) and patients with PBC (n = 18). (D) Representative flow cytometry plots of *ex vivo* expansion of PDC-E2$_{159-167}$-specific cells in paired intrahepatic CD103$^-$ and CD103$^+$ T_{RM} cells from HLA-A*0201$^+$ patients with PBC, stained with CFSE and PDC-E2$_{159-167}$ tetramer. (E) Precursor frequency of PDC-E2-specific CD8$^+$ T cells in paired intrahepatic CD103$^-$ and CD103$^+$ T_{RM} cell subsets (n = 10). (F) Relative proportions of CD103$^-$ and CD103$^+$ cells in total PDC-E2–specific reactive CD69$^+$CD8$^+$ T cells (n = 10). (G) CD103$^-$ and CD103$^+$ T_{RM} cells from patients with PBC were stimulated with a mix of PDC-E2 peptides for 6 h. The percentage of IFN-γ^+ or granzyme-B$^+$ cells in each subpopulation was analyzed (n = 10). (H) IFN-γ concentration in culture supernatants upon PDC-E2 peptides stimulation. Mean ± SEM. *p <0.05, **p <0.01, ***p <0.001, ****p <0.0001. Mann-Whitney *U* test (A-C), Wilcoxon matched-pairs test (E-H). CFSE, carboxyfluorescein succinimidyl ester; E2 component of pyruvate dehydrogenase; HCs, healthy controls; HLA, human leukocyte antigen; IFN, interferon; MFI, mean fluorescence intensity; PBC, primary biliary cholangitis; PDC-E2, E2 component of pyruvate dehydrogenase; T_{RM} cells, tissue-resident memory T cells.

immunofluorescence co-staining of CD8, CD69, CD103 and CK7 (Fig. 2A). The numbers of CD103$^+$CD8$^+$ cells in the portal area in PBC were significantly higher than in HCs and other chronic liver diseases (Fig. 2B). In treatment-naive patients with PBC, either absolute numbers (Fig. 2C) or percentages among CD8$^+$ cells (Fig. S2A) of portal area-infiltrating CD103$^+$CD8$^+$ cells positively correlated with biochemical parameters, including serum levels of alkaline phosphatase (ALP), gamma-glutamyltransferase and total bilirubin. No statistical correlation was observed between CD103$^+$CD8$^+$ cell numbers or frequencies and serum alanine aminotransferase, aspartate aminotransferase, IgM and IgG (Fig. S2B-C). For histological indices, portal-infiltrating CD103$^+$CD8$^+$ cell numbers (Fig. 2D) and frequencies (Fig. S2D) were both positively correlated with degree of hepatic inflammation and fibrosis stage. Interestingly, patients who responded to UDCA had significantly lower numbers and percentages of baseline CD103$^+$CD8$^+$ cells compared to those who were non-responders (Fig. 2E).

CD103$^+$ T_{RM} cells localize near biliary epithelial cells and are cytotoxic in PBC

To examine the spatial relationship between BECs and T_{RM} cells, we conducted nearest-neighbor analysis of CD103$^-$ T_{RM} (CD69$^+$CD103$^-$CD8$^+$) cells or CD103$^+$ T_{RM} (CD69$^+$CD103$^+$CD8$^+$) cells with respect to CK7$^+$ BECs (Fig. 2F). The average distance to the nearest BECs from CD103$^+$ T_{RM} cells was significantly lower than that from CD103$^-$ T_{RM} cells (Fig. 2G), and was also lower than CD103$^+$ T_{RM} cells from HCs or other liver diseases (Fig. S2E-

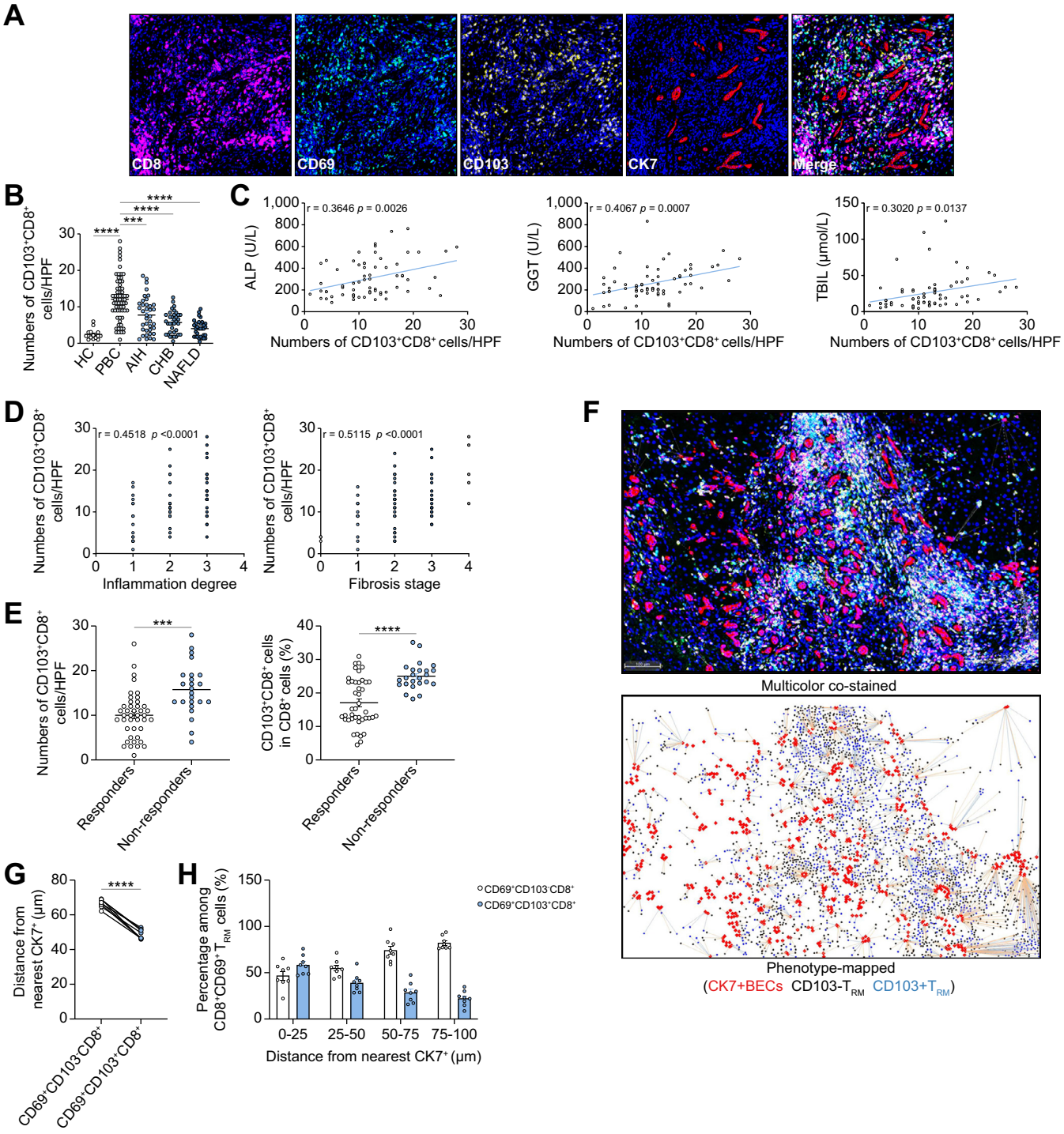

Fig. 2. Correlation of CD103$^+$ T_{RM} cells with the clinical and histological indices in PBC. (A) Representative multiplex co-staining of CD8, CD69, CD103 and CK7(×200) in PBC liver. (B) Quantification of portal area-infiltrating CD103$^+$CD8$^+$ cells in the livers of HCs (n = 15) and patients with PBC (n = 66), AIH (n = 38), CHB (n = 36) and NAFLD (n = 32). (C and D) Numbers of CD103$^+$CD8$^+$ cells positively correlated with serum ALP, GGT, TBIL levels (C) or hepatic inflammation degree and fibrosis stage (D) in patients with PBC (n = 66). (E) UDCA responders (n = 42) exhibited lower absolute numbers and percentages of CD103$^+$CD8$^+$ cells than non-responders (n = 24). (F) Representative multiplex co-staining (above) and its phenotype-mapped image (below) with CK7$^+$ (red) and T_{RM} cells (black dots, CD69$^+$CD103$^-$CD8$^+$ cells; blue dots, CD69$^+$CD103$^+$CD8$^+$ cells). (G) The average distance to the nearest BECs from CD103$^+$ T_{RM} cells was significantly lower than that from CD103$^-$ T_{RM} cells. (H) Spatial localization of CD103$^-$ T_{RM} cells and CD103$^+$ T_{RM} cells within different distances from nearest CK7$^+$ BECs. Mean ± SEM. ***p <0.001, ****p <0.0001. Student's t test (B, E), Spearman correlation test (C-D), paired t test (E-H). AIH, autoimmune hepatitis; ALP, alkaline phosphatase; BECs, biliary epithelial cells; CHB, chronic hepatitis B; GGT, Gamma-glutamyl transferase; HPF, high-power field; NAFLD, non-alcholic fatty liver disease; PBC, primary biliary cholangitis; TBIL, total bilirubin; UDCA, ursodeoxycholic acid.

G). Within close proximity (0–25 μm) to BECs, the frequency of CD103$^+$ T_{RM} cells was higher than that of CD103$^-$ T_{RM} cells. In contrast, CD8$^+$ T cells localized further from BECs were more enriched with CD103$^-$ T_{RM} cells (Fig. 2H).

These results led us to further confirm the direct cytotoxicity of T_{RM} cells against BECs, we established the 3D organoid co-culture system containing intrahepatic cholangiocytes and T cells. CD103$^+$ T_{RM} cells derived from patients with PBC produced significantly higher degranulation when co-cultured with autologous cholangiocytes (Fig. 3A), which was not observed in HCs or disease controls (Fig. S3A). Blocking assays demonstrated that cholangiocyte growth arrest and apoptosis caused by T_{RM} cell killing were mediated by both Fas/FasL-dependent and perforin/granzymeB-dependent pathways, with the latter being dominant (Fig. 3B-D). Confocal 3D reconstructions showed granzyme-B$^+$/perforin-positive T_{RM} cells accumulate around the damaged cholangiocyte organoids in the co-culture system (supplementary movie 1). Consistently, in portal areas of PBC livers, most CD103$^+$ T_{RM} cells close to the BECs were positive for granzyme-B and/or perforin (Fig. 3E; larger fields of view are shown in Fig. S3C). In addition to 3D organoid co-culture, similar results were also observed in planar co-culture of T_{RM} cells and autologous primary cholangiocytes (Fig. S3D-E).

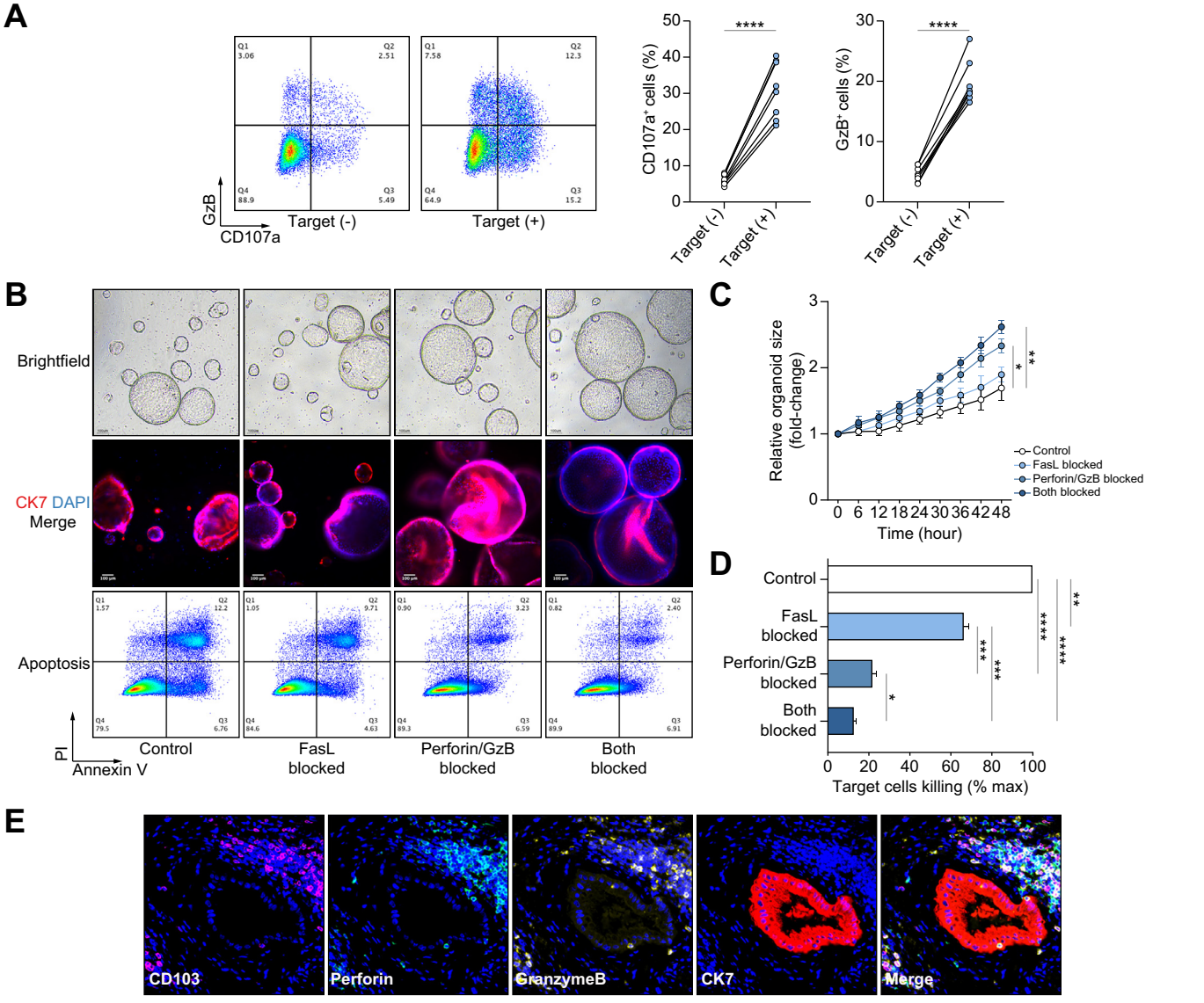

Fig. 3. CD103$^+$ T_{RM} cells present cytotoxicity against cholangiocytes in PBC. (A) Representative flow cytometry plots showing degranulation (CD107a and granzyme-B measured by flow cytometry) of CD103$^+$ T_{RM} cells (derived from patients with PBC) cultured with and without autologous cholangiocytes as target cells. (B) Representative bright-field microscopy images showing morphology of cholangiocyte organoid-T cell co-culture systems (Top row); Representative CK7/DAPI immunofluorescence co-staining (Middle row) and apoptosis measured by Annexin V/PI of cholangiocytes (Bottom row). (C) Size of cholangiocyte organoids during co-culture in the presence of specific inhibitors/antibodies of cytotoxic pathways. (D) Residual cytotoxicity against autologous cholangiocytes of CD103$^+$ T_{RM} cells in the presence of specific inhibitors/antibodies of cytotoxic pathways. (E) Representative histological multiplex co-staining of CD103, granzyme-B, Perforin and CK7(×400) in liver portal area of PBC. Mean ± SEM. $^*p$ <0.05, $^{**}p$ <0.01, $^{***}p$ <0.001, $^{****}p$ <0.0001. Wilcoxon matched-pairs test (A). Mann-Whitney *U* test (C-D). DAPI, 4,6-Diamidine-2-phenylindole; PBC, primary biliary cholangitis; PI, propidium iodide.

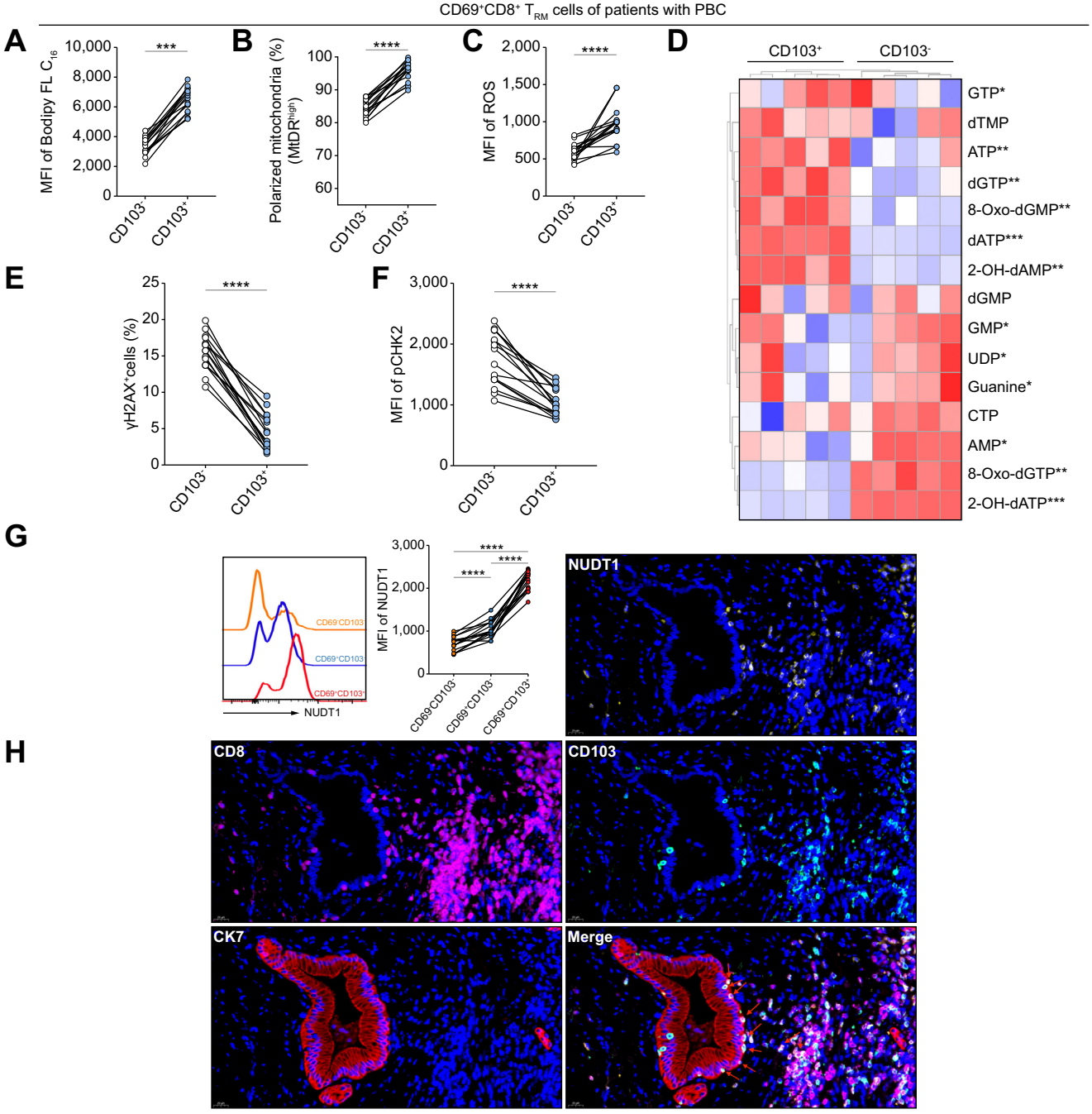

Fig. 4. Mitochondrial metabolic reprogramming and oxidative DNA damage response of CD103$^+$ T_{RM} cells is orchestrated by NUDT1 in PBC. (A-C) Exogenous fatty acid uptake, active mitochondria and intracellular ROS levels in CD103$^-$ and CD103$^+$ T_{RM} cells from patients with PBC (n = 16) monitored by Bodipy-FL-C_{16}, Mt-DR and Cell-ROX Reagent, respectively. (D) Relative quantification of nucleotide metabolites in paired CD103$^-$ and CD103$^+$ T_{RM} cells from patients with PBC (n = 5). (E and F) DNA double strand breaks assessed by phosphorylated activation of γ-H2AX (E) and CHK2 (F) in CD103$^-$ and CD103$^+$ T_{RM} cells from patients with PBC (n = 16). (G) NUDT1 expression among different intrahepatic CD8$^+$ T-cell subsets from patients with PBC (n = 16). (H) Representative multiplex co-staining of CD8, CD103, NUDT1 and CK7(400×) showing the juxtaposition of NUDT1-expressing CD103$^+$ T_{RM} cells and the damaged interlobular bile ducts. Mean ± SEM. $^*p$ <0.05, $^{**}p$ <0.01, $^{***}p$ <0.001, $^{****}p$ <0.0001. Wilcoxon matched-pairs test (A-G). Bodipy, boron dipyrromethene dyes; CHK2, checkpoint kinase 2; MFI, mean fluorescence intensity; Mt-DR, Mito-Tracker Deep Red; NUDT1, nucleoside diphosphate X hydrolase 1; PBC, primary biliary cholangitis.

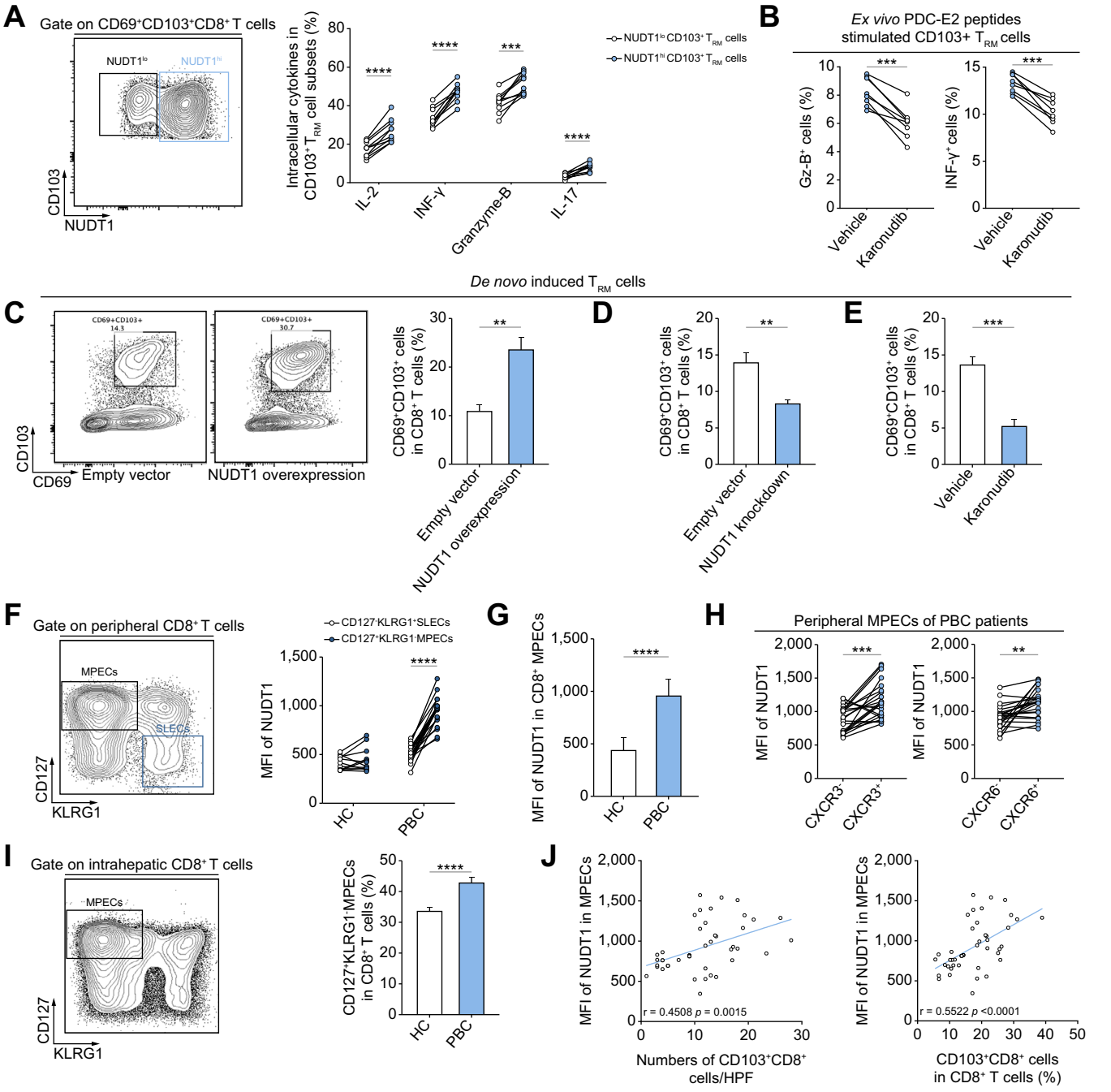

Fig. 5. NUDT1 promotes the function and phenotype of CD103$^+$ T_{RM} cells in PBC. (A) Cytokine-producing cell percentages in NUDT1^{low} and NUDT1^{high} CD103$^+$ T_{RM} subpopulations from patients with PBC (n = 10). (B) CD103$^+$ T_{RM} cells were stimulated with a mix of PDC-E2 peptides for 6 h in the presence of Karonudib (NUDT1 inhibitor) or vehicle control (n = 8). The percentage of IFN-γ^+ or granzyme-B$^+$ cells was analyzed. (C-E) Peripheral CD8$^+$ T cells were sequentially exposed with 3-day TCR engagement (0.25 μg/ml αCD3/28) followed by 3-day TGFβ (50 ng/ml) to induce tissue-resident phenotype *in vitro*. Induced CD69$^+$CD103$^+$ cell frequencies in CD8$^+$ T cells were increased by NUDT1 overexpression (C), and decreased by NUDT1 knockdown (D) or Karonudib treatment (E). (F) NUDT1 expression in paired peripheral CD8$^+$ MPECs and SLECs from patients with PBC and HCs. (G) Elevated NUDT1 expression in peripheral MPECs of patients with PBC compared with HCs. (H) NUDT1 expression in paired peripheral CXCR3$^-$/CXCR3$^+$ or CXCR6$^-$/CXCR6$^+$ MPECs from patients with PBC. (I) Frequency of liver-infiltrating MPECs from HCs (n = 15) and patients with PBC (n = 18). (J) NUDT1 expression in peripheral MPECs were positively correlated with the absolute numbers and frequencies of CD103$^+$CD8$^+$ cells in PBC liver tissues. Mean ± SEM. $^*p$ <0.05, $^{**}p$ <0.01, $^{***}p$ <0.001, $^{****}p$ <0.0001. Wilcoxon matched-pairs test (A, B, F, H), Mann-Whitney *U* test (C-E, G, I), Spearman correlation test (J). IFN, interferon; MFI, mean fluorescence intensity; MPECs, memory precursor effector cells; NUDT1, nucleoside diphosphate X hydrolase 1; PBC, primary biliary cholangitis; PDC-E2, E2 component of pyruvate dehydrogenase; SLECs, short-lived effector cells.

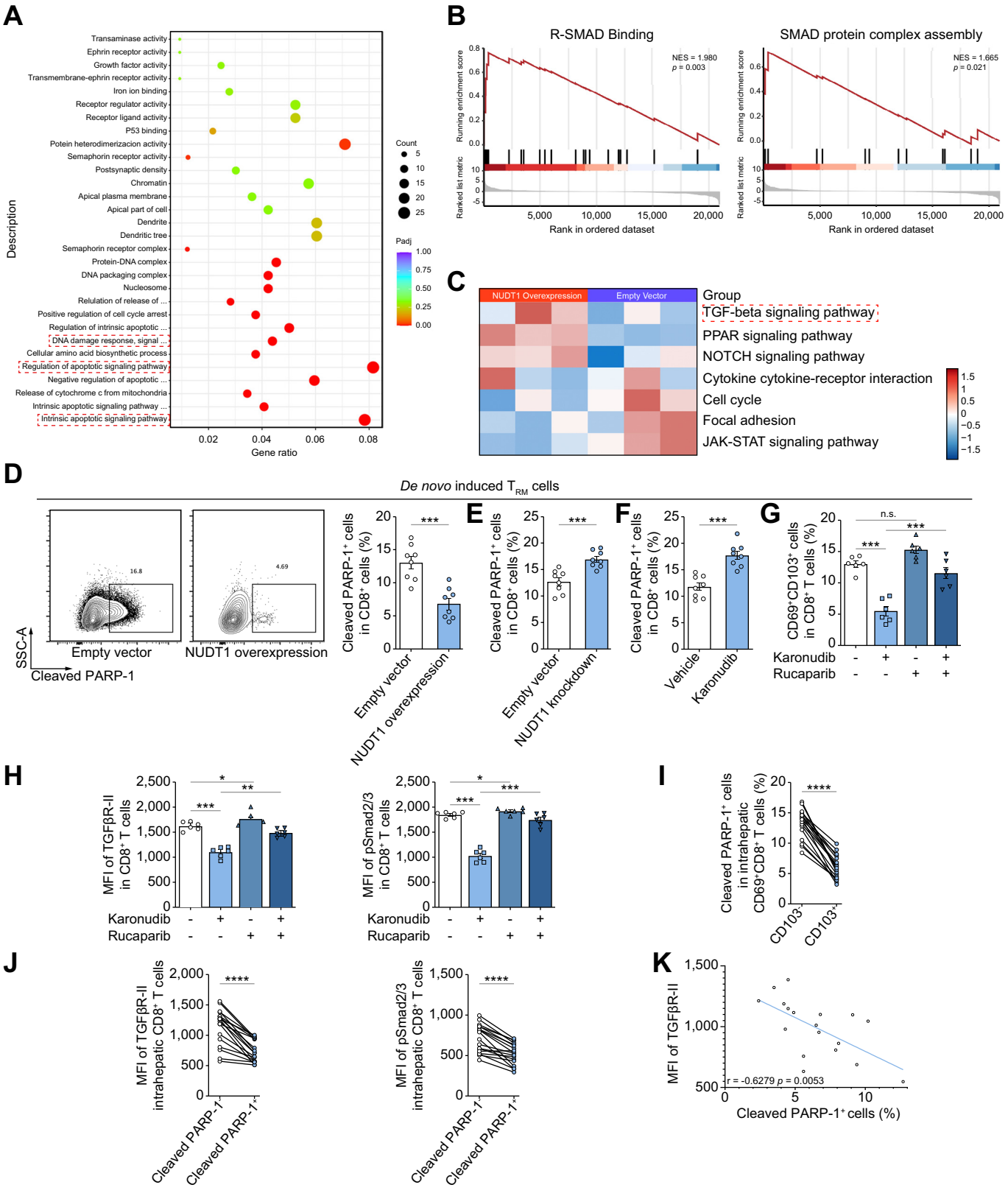

Fig. 6. NUDT1-dependent DNA damage resistance potentiates CD8⁺ T-cell residency upon activation via PARP1-TGFβ signaling *in vitro*. (A-C) RNA was extracted from NUDT1-overexpressing and control CD8⁺ T cells on the 6th day of tissue-residency *de novo* induction and subjected to RNA-seq (n = 3). Gene ontology enrichment analysis (A and B) and gene set variation analysis based on KEGG pathway database (C) indicating the DEGs. (D-F) Levels of cleaved PARP-1 in CD8⁺ T cells were decreased by NUDT1 overexpression (D) and increased by NUDT1 knockdown (E) or Karonudib (NUDT1 inhibitor) treatment (F). (G-H) 1 μM Karonudib or vehicle control was added to the culture media concomitantly with TCR engagement, with or without pretreatment of 0.5 μM Rucaparib (PARP1

CD103$^+$ T_{RM} cells within PBC livers accumulate high levels of ROS, but exhibit decreased dNTP pool oxidation and subsequent DNA damage

Persistent antigenic stimulation impairs mitochondrial oxidative phosphorylation (OXPHOS) and results in functional exhaustion or replicative senescence in T cells.[19,20] While T_{RM} cells within different tissues are reported to utilize increased mitochondrial β-oxidation to support their longevity.[21,22] CD103$^+$ T_{RM} cells demonstrated more fatty acid internalization (Fig. 4A) and higher mitochondrial respiratory activity (Fig. 4B) compared with the CD103$^-$ T_{RM} subset in PBC. Oxygen consumption rate analysis showed mitochondrial respiratory capacity was also higher in CD103$^+$ T_{RM} cells (Fig. S4A). Consistently, higher reactive oxygen species (ROS) production was observed in CD103$^+$ T_{RM} cells in PBC (Fig. 4C), which was also higher than CD103$^+$ T_{RM} cells isolated from controls (Fig. S4B).

Liquid chromatography-mass spectrometry analysis revealed a significant difference in their nucleotide metabolism. Strikingly, oxidized dNTPs, especially 8-hydroxy-dGTP and 2-hydroxy-dATP, were substantially lower in CD103$^+$ T_{RM} cells (Fig. 4D). Insertion of oxidized dNTPs into the genome leads to a DNA damage response (DDR). Consistently, indicators of DNA double-strand breaks, including γ-H2AX and pCHK2, showed that CD103$^+$ T_{RM} cells had a lower DDR level (Fig. 4E-F). Accordingly, we detected the expression of NUDT1, the key enzyme degrading oxidized purine dNTPs in mammalian cells; flow cytometry analysis demonstrated that NUDT1 was selectively upregulated in CD103$^+$ T_{RM} cells, rather than other counterparts in PBC (Fig. 3G). Furthermore, CD103$^+$ T_{RM} cells expressed higher NUDT1 than CD103$^+$ T_{RM} cells isolated from HCs or disease controls (Fig. S4C). Immunofluorescence co-staining of NUDT1, CD8, CD103 and CK7 in PBC livers confirmed high NUDT1 expression of CD103$^+$ T_{RM} cells in close proximity to or even within the damaged interlobular bile ducts (Fig. 3H).

NUDT1 regulates the function and intrahepatic accumulation of CD103$^+$ T_{RM} cells in PBC

Next, we investigated whether NUDT1 regulates the effector function of CD103$^+$ T_{RM} cells in PBC. Intracellular co-staining was performed for the comparison of NUDT1^{low} with NUDT1^{high} CD103$^+$ T_{RM} cell subpopulations. NUDT1^{high} CD103$^+$ T_{RM} cells expressed increased granzyme-B, IFN-γ, IL-2, and IL-17 (Fig. 5A), as well as exhibiting significantly higher Ki-67, TCF-1 (Fig. S4D). Upon re-stimulation with PDC-E2 peptides or anti-CD3/28, Karonudib (NUDT1 inhibitor) suppressed cytokine production from the CD103$^+$ subset (Fig. 5B; Fig. S5A), but not from the CD103$^-$ subset (Fig. S4E). In stark contrast, such effects were not observed in IL-15 or IL-12+IL-18 stimulated bystander-activated CD103$^+$ T_{RM} cells (Fig. S5B-C).

We next utilized a well-established T_{RM} cell *de novo* induction system to examine if the tissue-residency imprinted on peripheral CD8$^+$ T cells is regulated by NUDT1[13,23,24] (Fig. 5C). Lentivirus-mediated NUDT1 overexpression significantly increased the frequency (Fig. 5C) and cytokine production (Fig. S5D) of *de novo* induced CD69$^+$CD103$^+$CD8$^+$ cells, whereas NUDT1 knockdown (Fig. 4D; Fig. S5E) or Karonudib treatment (Fig. 5E; Fig. S5F) resulted in the opposite effect. Consistently, Karonudib rescued the cholangiocytes from growth defects and apoptosis induced by co-cultured autologous T_{RM} cells (Fig. S5G-H). In addition, NUDT1 overexpression increased the oxygen consumption rate of CD8$^+$ T cells after tissue-residency induction (Fig. S5I), either NUDT1 knockdown (Fig. S5J) or Karonudib (Fig. S5K) decreased their mitochondrial respiratory capacity.

Based on differential KLRG1 and CD127 expression, we distinguish peripheral CD8$^+$ short-lived effector cells (CD127$^-$KLRG1$^+$) from memory precursor effector cells (MPECs, CD127$^+$KLRG1$^-$) (Fig. 5F), the latter has been reported to be the dominant precursor cell source of T_{RM} cell replenishment within different tissues.[25–27] Significantly higher NUDT1 expression in peripheral MPECs than short-lived effector cells was observed in patients with PBC, but not in HCs (Fig. 5F). MPECs in patients with PBC exhibited higher NUDT1 expression than those in HCs (Fig. 5G). In addition, upregulated NUDT1 was observed in circulating MPECs expressing CXCR3 and CXCR6, which mediate hepatic T-cell recruitment and residence (Fig. 5H). As expected, the frequencies of intrahepatic MPECs (potential T_{RM} cell precursors) in PBC were significantly higher than those in HCs (Fig. 5I). Of note, the mean fluorescence intensity of NUDT1 in circulating MPECs positively correlated with the percentage of CD103$^+$ T_{RM} cells in paired liver tissue specimens (Fig. 5J).

In summary, NUDT1 maintains the effector functions of CD103$^+$ T_{RM} cells during autoantigen recall response in PBC, and also promotes their hepatic accumulation by imprinting a tissue-residency phenotype on their circulating precursor counterparts.

NUDT1-dependent DNA damage resistance potentiates CD8$^+$ T-cell residency via the PARP1-TGFβ-Smad axis *in vitro*

To further understand the mechanisms whereby NUDT1 promotes CD103$^+$ T_{RM} cell programming, we compared transcriptomes between NUDT1-overexpressing and control *de novo* induced T_{RM} cells using RNA-sequencing analysis. A gene ontology enrichment analysis revealed that the genes associated with DDR were downregulated in the NUDT1-overexpressing group (Fig. 6A), consistent with the known functions of NUDT1 in modulating resistance to oxidative DNA damage[28,29]; while the most critical events in TGFβ-Smad signaling including R-smad binding and smad protein-complex assembly were substantially upregulated by NUDT1 overexpression (Fig. 6B). Gene set variation analysis based on the KEGG pathway database also highlighted the increased levels of TGFβ signaling in the NUDT1-overexpressing group (Fig. 6C; Fig. S6A). Thus, we hypothesized that NUDT1-dependent DNA damage resistance would contribute to CD103$^+$ T_{RM} cell development or maintenance via upregulation of TGFβ-Smad signaling.

Recent studies showed that poly (ADP-ribose) polymerase-1 (PARP1), a central player in several different DDR pathways, can regulate the expression of TGFβ receptors and downstream

inhibitor) 6 h before TCR engagement. Induced CD69$^+$CD103$^+$ cell frequency (G), MFI of TGFβRII and pSmad2/3 (H) in CD8$^+$ T cells in different groups were analyzed. (I) Cleaved PARP-1 in CD103$^-$ and CD103$^+$ T_{RM} cells from patients with PBC (n = 18). (J) MFI of TGFβRII and pSmad2/3 in cleaved PARP-1$^-$ and cleaved PARP-1$^+$ CD8$^+$ T cells from patients with PBC (n = 18). (K) TGFβRII expression was negatively correlated with cleaved PARP-1$^+$ proportions in CD8$^+$ T cells. Mean ± SEM. $^*p$ <0.05, $^{**}p$ <0.01, $^{***}p$ <0.001, $^{****}p$ <0.0001. Mann-Whitney *U* test (C-E, G, I), Wilcoxon matched-pairs test (I-J), Spearman correlation test (K). DEGs, differentially expressed genes; KEGG, kyoto encyclopedia of genes and genomes; NUDT1, nucleoside diphosphate X hydrolase 1; PARP1, poly (ADP-ribose) polymerase-1.

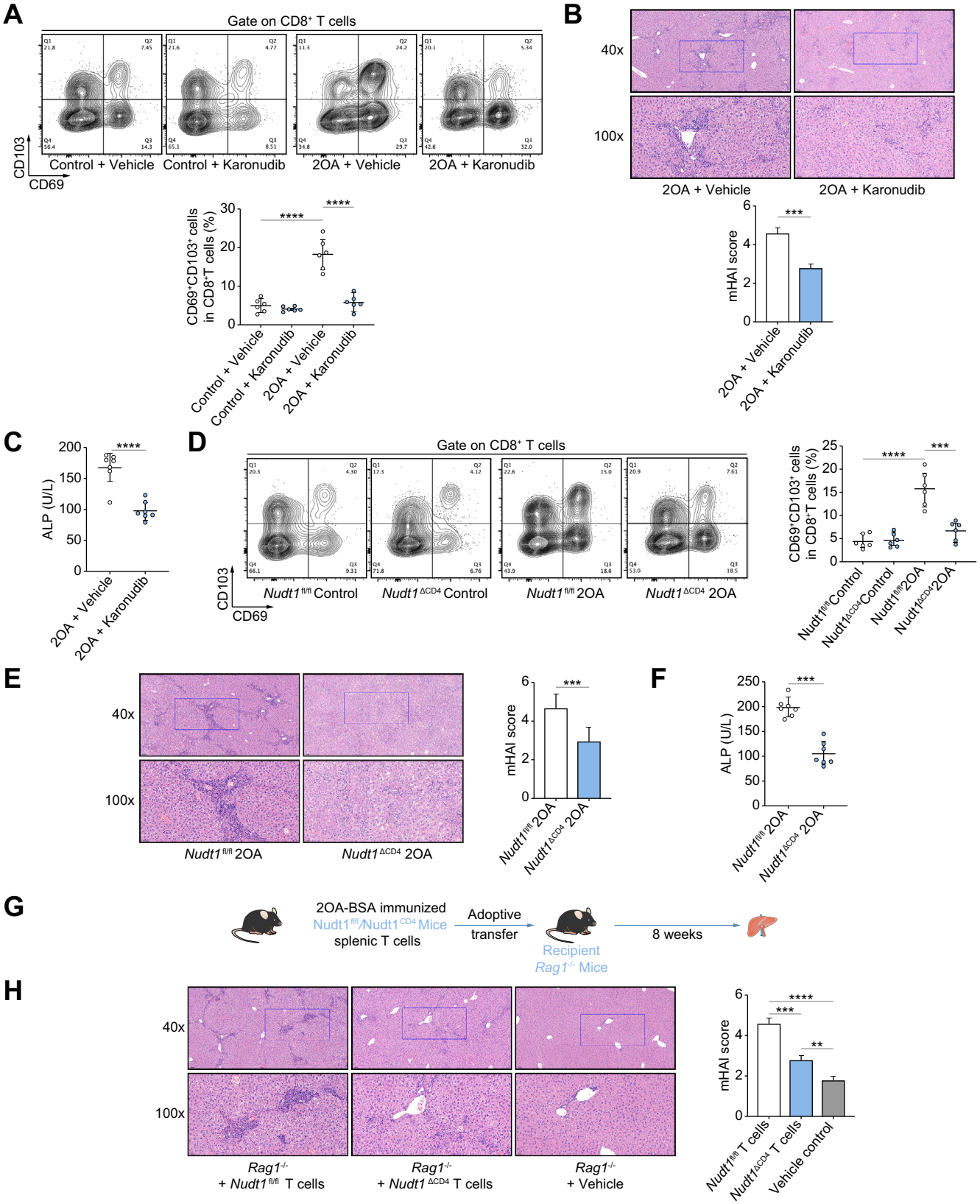

Fig. 7. Pharmacological blockade or genetic deletion of NUDT1 eliminates CD103$^+$ T_{RM} cells *in vivo*. (A-F) Liver tissues and liver-infiltrating lymphocytes were collected 12 weeks after primary 2OA-BSA immunization. (A) Liver-infiltrating CD69$^+$CD103$^+$ cell frequency in CD8$^+$ T cells from mice immunized with 2OA or control under Karonudib or vehicle control treatment. (B) Representative H&E staining of liver portal areas and the mHAI score of the liver from indicated mice.

smad signaling in T cells.[30,31] As expected, the percentage of cleaved PARP1 (the active fragment cleavage of PARP1)-positive cells was reduced in NUDT1-overexpressing $CD8^+$ T cells compared to controls (Fig. 6D). In contrast, either NUDT1 knockdown (Fig. 6E) or NUDT1 inhibitor treatment (Fig. 6F) increased the level of cleaved PARP1. Pretreatment with an inhibitor (Rucaparib) of PARP1 reversed the reduction in $CD103^+$ T_{RM} cell frequency induced by Karonudib (Fig. 6G); all other tested inhibitors of different DDR signaling proteins (including DNA-dependent protein kinase catalytic subunit, ATM, ATR, CHK1 and Wee1) fail to rescue it (Fig. S6D-H). Furthermore, Rucaparib pretreatment restored the inhibitory effect of Karonudib on TGFβRII and phospho-Smad2/3 expression upon TCR/TGFβ sequential exposure (Fig. 6H), but not under IL15/TGFβ sequential induction (Fig. S6C). Finally, we validated this PARP1-TGFβ-Smad axis in liver-infiltrating $CD8^+$ T cells from patients with PBC; $CD103^+$ T_{RM} cells showed a lower level of cleaved PARP1 than the $CD103^-$ T_{RM} subset (Fig. 6I) and cleaved $PARP1^+$ $CD8^+$ T cells displayed lower expression of TGFβRII and phospho-Smad2/3 (Fig. 6J). Moreover, either TGFβRII (Fig. 6K) or phospho-Smad2/3 expression (Fig. S6I) was negatively correlated with cleaved $PARP1^+$ proportions in $CD8^+$ T cells.

Overall, NUDT1-dependent DNA damage resistance upregulates TGFβ-Smad signaling by preventing PARP1 hyperactivation, thus promoting $CD103^+$ T_{RM} cell programming in PBC.

Inhibition of NUDT1 eliminates $CD103^+$ T_{RM} cells and attenuates 2OA-BSA-induced cholangitis *in vivo*

To examine the potential impact of NUDT1 on $CD103^+$ T_{RM} cells and their roles in PBC development *in vivo*, we induced cholangitis in mice immunized with BSA-conjugated 2OA as described.[2] Liver-infiltrating $CD69^+CD103^+CD8^+$ T_{RM} cell frequency was significantly increased in 2OA-immunized mice, and was specifically eliminated by Karonudib oral gavage (Fig. 7A). Liver inflammation (Fig. 7B) and serum ALP levels (Fig. 7C) in 2OA-immunized mice were significantly decreased by Karonudib. After being immunized with 2OA for 12 weeks, T cell-specific NUDT1-deficient *Nudt1*$^{\triangle CD4}$ mice developed a considerably lower $CD103^+$ T_{RM} cell frequency compared with $NUDT1^{fl/fl}$ control littermates (Fig. 7D), accompanied by the alleviation of portal inflammation (Fig. 7E) and decrease in serum ALP (Fig. 7F). Splenic pan-T cells from 2OA-immunized *Nudt1*$^{\triangle CD4}$ or *Nudt1*$^{fl/fl}$ mice were purified and adoptively transferred into *Rag1*$^{-/-}$ mice (Fig. 7G); HE staining revealed that NUDT1 knockdown in T cells led to decreased cholangitis in a cell-autonomous fashion (Fig. 7H).

NUDT1 promoted longevity of $CD103^+$ T_{RM} cells during cholangitis in a PARP1-dependent manner

To further confirm if NUDT1 promotes the long-term residency phenotype of $CD8^+$ T cells *in vivo*, an adoptive cell co-transfer experiment was performed. Pan-T cells were isolated from the spleens of wild-type CD45.1 mice and *Nudt1*$^{\triangle CD4}$-CD45.2 mice after 4-week 2OA-immunization, reactivated *in vitro* and then adoptively co-transferred into 6-week-old *Rag1*$^{-/-}$ recipient mice. Recipients were sacrificed on the indicated date and liver-infiltrating lymphocytes were collected for flow cytometry analysis (Fig. 8A). NUDT1 deficiency led to a progressive loss of $CD103^+$ T_{RM} cells over time (Fig. 8B), but only had a slight effect on total liver-infiltrating $CD8^+$ cell frequency (Fig. 8C).

Next, to investigate if the mechanism by which NUDT1 promotes $CD103^+$ T_{RM} cell longevity also relies on PARP1, Karonudib or vehicle oral gavage were performed in 2OA-immunized *Parp1*$^{-/-}$ mice and wild-type littermates. Karonudib failed to abrogate $CD103^+$ T_{RM} cells in *Parp1*$^{-/-}$ mice after immunization with 2OA-CFA for 12 weeks (Fig. 8D). Pharmacological inhibition of PARP1 activity by Rucaparib also restored the frequency of $CD103^+$ T_{RM} cells, as well as their TGFβRII and phosphor-Smad2/3 expression (Fig. 8E). In addition, Rucaparib treatment also partially restored the frequency of $KLRG1^{low}CD127^{high}$ MPECs in NUDT1-deficient T cells (Fig. S7A-B).

Taken together, genetic ablation or pharmacological blockade of PARP1 restored NUDT1-deficient $CD103^+$ T_{RM} cell longevity during 2OA-induced cholangitis and skewed the T_{RM} cells towards a long-lived MPEC phenotype.

Discussion

Liver-infiltrating PDC-E2-specific memory $CD8^+$ T cells play a leading role in biliary destruction in PBC progression. However, phenotypic and functional characterization of effector $CD8^+$ T cells in PBC have been primarily confined to peripheral blood. In this study, we have comprehensively studied intrahepatic $CD103^+$ T_{RM} cells, with respect to their autoantigen-specificity, near-BECs localization and cytotoxicity against BECs. We also suggest that their antigen-dependent hyperactivation, and the longevity phenotype are based upon NUDT1.

We previously proposed that residual $CD103^+$ T_{RM} cells may trigger a robust and rapid recall response, resulting in recurrence of liver inflammation in patients with autoimmune hepatitis discontinuing glucocorticoid treatment.[24] In the present study, we found an apparent link between baseline $CD103^+$ T_{RM} cell numbers and response to UDCA in PBC. Hence, $CD103^+$ T_{RM} cells may reflect the underlying disease state, severity or prognosis, since UDCA response is regarded as a disease-specific indicator for risk stratification and prognosis in PBC.[5,6]

We also demonstrated that $CD103^+$ T_{RM} cells account for the majority of PDC-E2-specific $CD8^+$ T lymphocytes and present direct cytotoxicity against BECs in PBC livers. This provides a plausible explanation for the organ specificity and chronicity of PBC, since the pathogenic $CD103^+$ T_{RM} cells exhibit a longevity phenotype and rarely dislodge from their residence sites once established. The data also suggests that future immune-based

(C) Serum ALP levels of indicated mice. (D) Liver-infiltrating $CD69^+CD103^+$ cell frequency from $NUDT1^{\triangle CD4}$ mice and $NUDT1^{fl/fl}$ control littermates immunized with 2OA or control. (E) Representative H&E staining of liver portal areas and the mHAI score of the liver from indicated mice. (F) Serum ALP levels of indicated mice. (G-H) T cells from $NUDT1^{\triangle CD4}$ or $NUDT1^{fl/fl}$ mice were adoptively transferred into 6-week-old *Rag1*$^{-/-}$ recipient mice; liver tissues were collected for histological evaluation 8-weeks post-transfer. (G) Workflow of the experimental procedure. (H) Representative H&E staining of liver sections from different recipients. Mean ± SEM. $^{**}p$ <0.01, $^{***}p$ <0.001, $^{****}p$ <0.0001. Mann-Whitney *U* test (A-H). ALP, alkaline phosphatase; mHAI, modified hepatitis activity index; NUDT1, nucleoside diphosphate X hydrolase 1; 2OA, 2-octynoic acid.

therapies of relapsed/refractory PBC could focus on the elimination of CD103$^+$ T_{RM} cells.

Persistent antigen stimulation limits the mitochondrial oxidative capacity of T cells.[19,32] Paradoxically, CD103$^+$ T_{RM} cells within different tissues utilize increased mitochondrial OXPHOS to support their longevity.[21] One of the detrimental effects of excess ROS derived from OXPHOS is oxidative DNA damage. We revealed CD103$^+$ T_{RM} cells within PBC livers accumulate high levels of ROS, but show decreased dNTP pool oxidation and subsequent DDR, in line with previous reports that liver CD103$^+$ T_{RM} cells have longevity phenotypes.[15,33] We noted that CD103$^+$ T_{RM} cells within PBC livers have higher expression of the enzyme NUDT1. By comparing the different functions of NUDT1^{low} and NUDT1^{high} CD103$^+$ T_{RM} subpopulations, together with a series of further *in vitro* experiments, we also identified that NUDT1 potentiates CD103$^+$ T_{RM} cell programming via PARP1-TGFβ-Smad

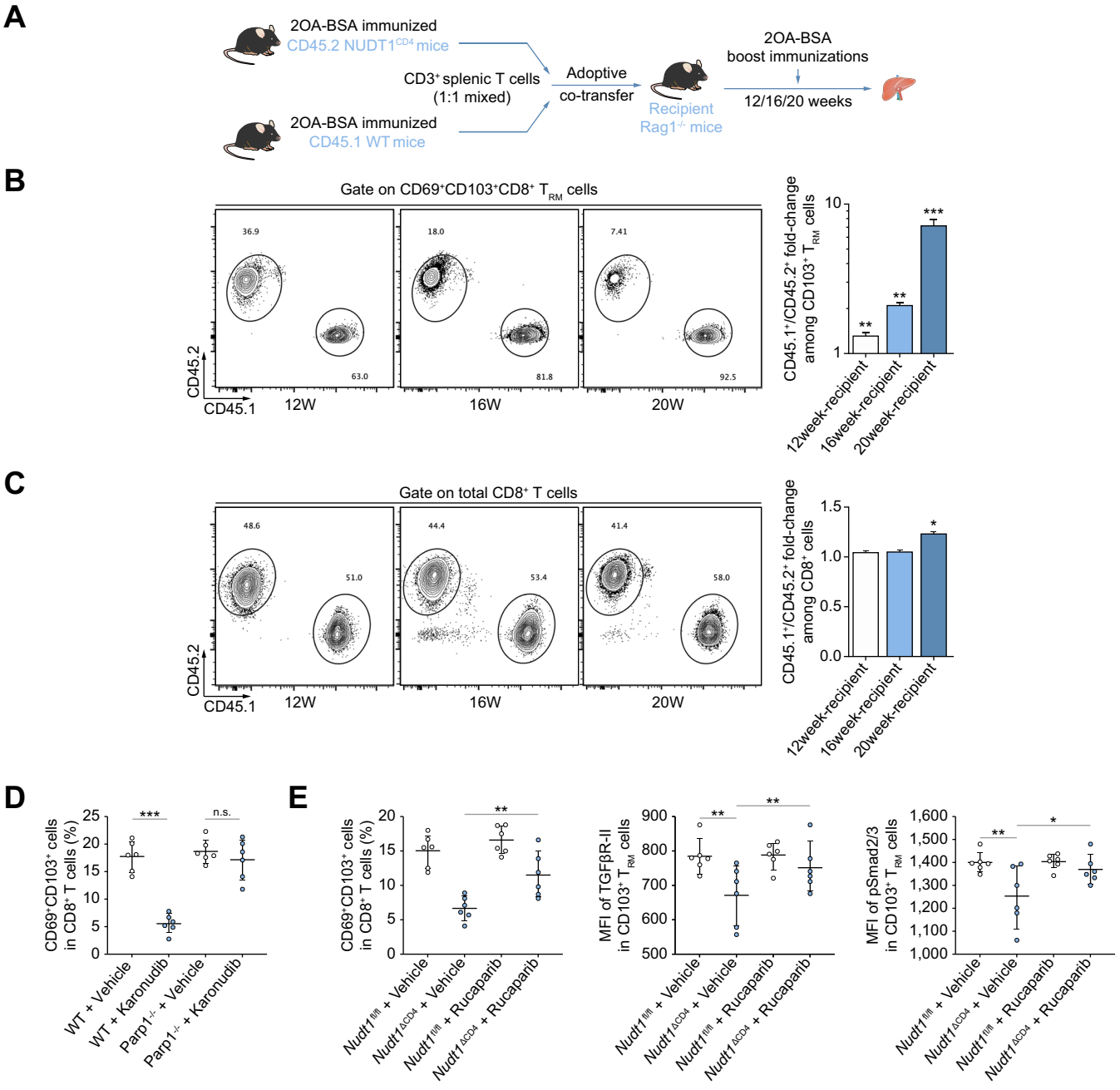

Fig. 8. NUDT1 promotes long-term survival of CD103$^+$ T_{RM} cells in a PARP1-dependent manner *in vivo*. (A-C) Pan-T cells were isolated from WT-CD45.1 mice and NUDT1$^{\triangle CD4}$-CD45.2 mice after 4-week 2OA-immunization, then mixed (1:1 ratio) and adoptively co-transferred into 6-week-old *Rag1*$^{-/-}$ recipients. Workflow of the experimental procedure is shown (A). Mean fold-change (±SEM; n = 5) in frequencies of CD45.1- or CD45.2-expressing CD103$^+$ T_{RM} cells (B) or total CD8$^+$ T cells (C) from recipients 12/16/20-weeks post-transfer. (D) Liver-infiltrating CD69$^+$CD103$^+$ cell frequency in CD8$^+$ T cells from 12-week 2OA-immunized *Parp1*$^{-/-}$ or WT littermates under Karonudib (NUDT1 inhibitor) or vehicle treatment. (E) Liver-infiltrating CD69$^+$CD103$^+$ cell frequency in CD8$^+$ T cells, MFI of TGFβRII and MFI of pSmad2/3 in CD103$^+$ T_{RM} cells from 12-week 2OA-immunized *Nudt1*$^{\triangle CD4}$ mice or *Nudt1*$^{fl/fl}$ littermates under Rucaparib or vehicle treatment. Mean ± SEM. **p* <0.05, ***p* <0.01, ****p* <0.001. Mann-Whitney *U* test (B-E). 2OA, 2-octynoic acid; MFI, mean fluorescence intensity; NUDT1, nucleoside diphosphate X hydrolase 1.

signaling. Adoptive co-transfer experiments revealed that NUDT1 not only promotes intrahepatic CD103$^+$ T_{RM} cell survival, but also skews T_{RM} cells towards a long-lived MPEC phenotype in a PARP1-dependent manner *in vivo*.

There remain limitations to our findings, including the fact that animal experiments cannot perfectly mirror the pathophysiology of human disease, especially the PBC-specific antigenic effects. Even so, we suppose that NUDT1, as the central hub of metabolic reprogramming and DDR, could be key to deciphering the heterogeneity of T_{RM} cells from an immunometabolism perspective.

The relationship between metabolic reprogramming, ROS production, NUDT1 activity and DDR signaling in T cell-driven autoimmunity remain controversial.[28] Meanwhile, cellular senescence characterized by morphological changes or DDR factor expression is an intrinsic feature of cholangiocytes and hepatocytes in PBC,[34,35] and has a detrimental role in biliary injury and impairment of liver regeneration.[34,35] Therefore, using broad-spectrum DNA-damaging targeted drugs may inflict further biliary damage in PBC. However, NUDT1 expression is extremely low in the hepatic parenchyma, suggesting reduced toxicity if it is inhibited.

In summary, we identified CD103$^+$ T_{RM} cells as the major fraction of PDC-E2-specific autoreactive CD8$^+$ T cells within PBC livers, while their inappropriate expansion, antigen-dependent hyperactivation and longevity phenotype were dependent on NUDT1 activity. On the basis of these investigations, we propose a new paradigm for therapeutic immune modulation in PBC, exploiting targeted manipulation of PARP1-centered DDRs, that regulate TGFβ signaling in CD103$^+$ T_{RM} cells. This approach allows for highly selective suppression of autoantigen-specific reactive T cells, displays clear therapeutic benefits, and has less off-target toxicity.

Abbreviations

2OA, 2-octynoic acid; ALP, alkaline phosphatase; BECs, biliary epithelial cells; CFSE, carboxyfluorescein succinimidyl ester; CTL, cytotoxic T lymphocyte; DDR, DNA damage response; HCs, healthy controls; OXPHOS, oxidative phosphorylation; MPECs, memory precursor effector cells; NUDT1, nucleoside diphosphate X hydrolase 1; PARP1, poly (ADP-ribose) polymerase-1; PBC, primary biliary cholangitis; PDC-E2, E2 component of pyruvate dehydrogenase; ROS, reactive oxygen species; T_{RM} cells, tissue-resident memory T cells; UDCA, ursodeoxycholic acid.

Financial support

This work was supported by the National Natural Science Foundation of China grants (#82130017 and 81830016 to XM, #81922010 and 81873561 to RT, #81900523 to YL, #81790634 and 82070581 to QW, #81800504 to ML, #81421001 to JF), Shanghai Science and Technology Innovation Action Plan of Shanghai Municipal Science and Technology Commission (#21ZR1438700 to WC) and the Innovative research team of high-level local universities in Shanghai (#SHSMU-ZLCX20211600).

Conflict of interest

The authors have no conflicting financial interests.

Please refer to the accompanying ICMJE disclosure forms for further details.

Authors' contributions

XM, MEG and ZY designed and supervised the study. XM and RT acquired funding. BH, ZY, ZL and QQ performed the experiments. BH, ZY, ZL, QQ, YC, YL, JL, YL, BL, JZ and RC collected samples and clinical information. BH, ZL, QQ, ZY, ZL, TH analyzed the data. BH drafted the manuscript. XM, MEG and ZY reviewed the manuscript.

Data availability statement

Data are available upon request from the corresponding author Dr. Xiong Ma.

Acknowledgement

We are grateful to all the participants who contributed to this study.

Supplementary data

Supplementary data to this article can be found online at https://doi.org/10.1016/j.jhep.2022.06.014.

References

Author names in bold designate shared co-first authorship

[1] Terziroli Beretta-Piccoli B, Mieli-Vergani G, Vergani D. The clinical usage and definition of autoantibodies in immune-mediated liver disease: a comprehensive overview. J Autoimmun 2018;95:144–158.
[2] Wakabayashi K, Lian ZX, Leung PS, Moritoki Y, Tsuneyama K, Kurth MJ, et al. Loss of tolerance in C57BL/6 mice to the autoantigen E2 subunit of pyruvate dehydrogenase by a xenobiotic with ensuing biliary ductular disease. Hepatology 2008;48:531–540.
[3] Kita H, Matsumura S, He XS, Ansari AA, Lian ZX, Van De Water J, et al. Quantitative and functional analysis of PDC-E2-specific autoreactive cytotoxic T lymphocytes in primary biliary cirrhosis. J Clin Invest 2002;109:1231–1240.
[4] Lleo A, Wang GQ, Gershwin ME, Hirschfield GM. Primary biliary cholangitis. Lancet 2020;396:1915–1926.
[5] Hirschfield GM, Beuers U, Corpechot C, Invernizzi P, Jones D, Marzioni M, et al. EASL Clinical Practice Guidelines: the diagnosis and management of patients with primary biliary cholangitis. J Hepatol 2017;67:145–172.
[6] Terziroli Beretta-Piccoli B, Mieli-Vergani G, Vergani D, Vierling JM, Adams D, Alpini G, et al. The challenges of primary biliary cholangitis: what is new and what needs to be done. J Autoimmun 2019;105:102328.
[7] **Zhu C**, **Boucheron N**, Müller AC, Májek P, Claudel T, Halilbasic E, et al. 24-Norursodeoxycholic acid reshapes immunometabolism in CD8(+) T cells and alleviates hepatic inflammation. J Hepatol 2021;75:1164–1176.
[8] Tsuda M, Ambrosini YM, Zhang W, Yang G-X, Ando Y, Rong G, et al. Fine phenotypic and functional characterization of effector cluster of differentiation 8 positive T cells in human patients with primary biliary cirrhosis. Hepatol (Baltimore, Md.) 2011;54:1293–1302.
[9] Beura LK, Mitchell JS, Thompson EA, Schenkel JM, Mohammed J, Wijeyesinghe S, et al. Intravital mucosal imaging of CD8 + resident memory T cells shows tissue-autonomous recall responses that amplify secondary memory article. Nat Immunol 2018;19:173–182.
[10] Park CO, Kupper TS. The emerging role of resident memory T cells in protective immunity and inflammatory disease. Nat Med 2015;21:688–697.
[11] Sun H, Sun C, Xiao W, Sun R. Tissue-resident lymphocytes: from adaptive to innate immunity. Cell Mol Immunol 2019;16:205–215.
[12] Topham DJ, Reilly EC. Tissue-resident memory CD8+ T cells: from phenotype to function. Front Immunol 2018;9.
[13] Pallett LJ, Davies J, Colbeck EJ, Robertson F, Hansi N, Easom NJW, et al. IL-2high tissue-resident T cells in the human liver: sentinels for hepatotropic infection. J Exp Med 2017;214:1567–1580.
[14] Swadling L, Pallett LJ, Maini MK. Liver-resident CD8+ T cells: learning lessons from the local experts. J Hepatol 2020;72:1049–1051.
[15] **Kim JH**, **Han JW**, Choi YJ, Rha M-S, Koh JY, Kim KH, et al. Functions of human liver CD69+CD103-CD8+ T cells depend on HIF-2α activity in healthy and pathologic livers. J Hepatol 2020;72:1170–1181.
[16] Kefalakes H, Horgan XJ, Jung MK, Amanakis G, Kapuria D, Bolte FJ, et al. Liver-resident bystander CD8(+) T cells contribute to liver disease pathogenesis in chronic hepatitis D virus infection. Gastroenterology 2021.

[17] Kim H-D, Jeong S, Park S, Lee YJ, Ju YS, Kim D, et al. Implication of CD69+CD103+ tissue-resident-like CD8+ T cells as a potential immunotherapeutic target for cholangiocarcinoma. Liver Int 2021;41:764–776.
[18] Barsch M, Salié H, Schlaak AE, Zhang Z, Hess M, Mayer LS, et al. T cell exhaustion and residency dynamics inform clinical outcomes in hepatocellular carcinoma. J Hepatol 2022.
[19] Vardhana SA, Hwee MA, Berisa M, Wells DK, Yost KE, King B, et al. Impaired mitochondrial oxidative phosphorylation limits the self-renewal of T cells exposed to persistent antigen. Nat Immunol 2020;21:1022–1033.
[20] Acerbi G, Montali I, Ferrigno GD, Barili V, Schivazappa S, Alfieri A, et al. Functional reconstitution of HBV-specific CD8 T cells by in vitro polyphenol treatment in chronic hepatitis B. J Hepatol 2021;74:783–793.
[21] Pan Y, Tian T, Park CO, Lofftus SY, Mei S, Liu X, et al. Survival of tissue-resident memory T cells requires exogenous lipid uptake and metabolism. Nature 2017;543:252–256.
[22] Varanasi SK, Kumar SV, Rouse BT. Determinants of tissue-specific metabolic adaptation of T cells. Cell Metab 2020;32:908–919.
[23] Swadling L, Pallett LJ, Diniz MO, Baker JM, Amin OE, Stegmann KA, et al. Human liver memory CD8+ T cells use autophagy for tissue residence. Cell Rep 2020;30:687–698.e6.
[24] **You Z**, **Li Y**, **Wang Q**, Zhao Z, Li Y, Qian Q, et al. The clinical significance of hepatic CD69+CD103+CD8+ resident-memory T cells in autoimmune hepatitis. Hepatology 2021;74:847–863.
[25] **Kurd NS**, **He Z**, Louis TL, Milner JJ, Omilusik KD, Jin W, et al. Early precursors and molecular determinants of tissue-resident memory CD8+ T lymphocytes revealed by single-cell RNA sequencing. Sci Immunol 2020;5.
[26] Kok L, Dijkgraaf FE, Urbanus J, Bresser K, Vredevoogd DW, Cardoso RF, et al. A committed tissue-resident memory T cell precursor within the circulating CD8+ effector T cell pool. J Exp Med 2020;217.
[27] Mani V, Bromley SK, Äijö T, Mora-Buch R, Carrizosa E, Warner RD, et al. Migratory DCs activate TGF-b to precondition naïve CD8+T cells for tissue-resident memory fate. Science 2019;366.
[28] Karsten S, Fiskesund R, Zhang X-M, Marttila P, Sanjiv K, Pham T, et al. MTH1 as a target to alleviate T cell driven diseases by selective suppression of activated T cells. Cell Death Differ 2021.
[29] Huber KV, Salah E, Radic B, Gridling M, Elkins JM, Stukalov A, et al. Stereospecific targeting of MTH1 by (S)-crizotinib as an anticancer strategy. Nature 2014;508:222–227.
[30] Lönn P, van der Heide LP, Dahl M, Hellman U, Heldin C-H, Moustakas A. PARP-1 attenuates smad-mediated transcription. Mol Cell 2010;40:521–532.
[31] Zhang P, Nakatsukasa H, Tu E, Kasagi S, Cui K, Ishikawa M, et al. PARP-1 regulates expression of TGF-β receptors in T cells. Blood 2013;122:2224–2232.
[32] **Scharping NE**, **Rivadeneira DB**, **Menk AV**, Vignali PDA, Ford BR, Rittenhouse NL, et al. Mitochondrial stress induced by continuous stimulation under hypoxia rapidly drives T cell exhaustion. Nat Immunol 2021;22:205–215.
[33] **Pallett LJ**, **Burton AR**, Amin OE, Rodriguez-Tajes S, Patel AA, Zakeri N, et al. Longevity and replenishment of human liver-resident memory T cells and mononuclear phagocytes. J Exp Med 2020;217:e20200050.
[34] Manco R, Clerbaux LA, Verhulst S, Bou Nader M, Sempoux C, Ambroise J, et al. Reactive cholangiocytes differentiate into proliferative hepatocytes with efficient DNA repair in mice with chronic liver injury. J Hepatol 2019;70:1180–1191.
[35] Ferreira-Gonzalez S, Lu WY, Raven A, Dwyer B, Man TY, O'Duibhir E, et al. Paracrine cellular senescence exacerbates biliary injury and impairs regeneration. Nat Commun 2018;9:1020.